MOLECULAR AND CELLULAR BIOLOGY, July 2007, p. 4980–4990 Vol. 27, No. 13
0270-7306/07/$08.00+0 doi:10.1128/MCB.02304-06

Depletion of Mammalian CCR4b Deadenylase Triggers Elevation of the *p27^{Kip1}* mRNA Level and Impairs Cell Growth▽

Masahiro Morita, Toru Suzuki, Takahisa Nakamura, Kazumasa Yokoyama, Takashi Miyasaka, and Tadashi Yamamoto*

Division of Oncology, Department of Cancer Biology, Institute of Medical Science, University of Tokyo, Tokyo 108-8639, Japan

Received 11 December 2006/Returned for modification 11 January 2007/Accepted 11 April 2007

The stability of mRNA influences the abundance of cellular transcripts and proteins. Deadenylases play critical roles in mRNA turnover and thus are important for the regulation of various biological events. Here, we report the identification and characterization of CCR4b/CNOT6L, which is homologous to yeast CCR4 mRNA deadenylase. CCR4b is localized mainly in the cytoplasm and displays deadenylase activity both in vitro and in vivo. CCR4b forms a multisubunit complex similar to the yeast CCR4-NOT complex. Suppression of CCR4b by RNA interference results in growth retardation of NIH 3T3 cells accompanied by elevation of both *p27^{Kip1}* mRNA and p27^{Kip1} protein. Reintroduction of wild-type CCR4b, but not mutant CCR4b lacking deadenylase activity, restores the growth of CCR4b-depleted NIH 3T3 cells. The data suggest that CCR4b regulates cell growth in a manner dependent on its deadenylase activity. We also show that *p27^{Kip1}* mRNA is stabilized and its poly(A) tail is preserved in CCR4b-depleted cells. Our findings provide evidence that CCR4b deadenylase is a constituent of the mammalian CCR4-NOT complex and regulates the turnover rate of specific target mRNAs. Thus, CCR4b may be involved in various cellular events that include cell proliferation.

Regulation of mRNA turnover rates is important in determining the abundance and translational efficiencies of mRNAs. Removal of the 3′ poly(A) tail triggers degradation of mRNAs. Two mechanisms have been described for the completion of mRNA degradation. With the first mechanism, a decapping complex consisting of Dcp1 and Dcp2 recognizes the deadenylated mRNA and hydrolyzes the m^{7}GpppN cap (5′ capping structure of mRNA), leading to 5′-to-3′ exonuclease digestion catalyzed by Xrn1. In the other mechanism, deadenylation is followed by 3′-to-5′ degradation of the deadenylated mRNA by the exosome complex containing 3′-to-5′ exonuclease. In either case, deadenylation is a critical step in mRNA degradation and regulates the abundance of mRNA (for reviews, see references 22 and 34).

Each mRNA has a distinct degradation rate. Although the precise mechanism of deadenylation remains to be established, the deadenylation rate of each mRNA would influence the mRNA degradation rate. Sequence elements that are responsible, at least in part, for mRNA turnover by promoting deadenylation have been identified in the c-Fos, interleukin 2, and tumor necrosis factor alpha genes (5, 12, 15). One of the best-studied and most prevalent elements is the AU-rich element (ARE), which is found in the 3′ untranslated region (3′ UTR) of mRNAs. AREs in the interleukin 2 mRNA and tumor necrosis factor alpha mRNA promote rapid deadenylation-dependent mRNA decay (5, 15). In addition, because the 3′ poly(A) tail can enhance translation, deadenylation influences the efficiency of translation (4, 23). Thus, deadenylases are crucial for gene expression and therefore are likely to be important for many biological processes.

Two distinct enzyme complexes, Pan2-Pan3 and CCR4-NOT, have been identified in yeast as mRNA deadenylases (for reviews, see references 22 and 34). The yeast Pan2-Pan3 protein complex consists of the Pan2 catalytic subunit and the Pan3 auxiliary factor. Yeast Pan2 is involved in an early step in mRNA deadenylation in which the long poly(A) tail is shortened to approximately 75 nucleotides (nt) (2). The yeast CCR4-NOT protein complex consists of CCR4, five NOT proteins (NOT1 to NOT5), CAF1, CAF40, and CAF130 (7, 8, 9). Yeast CCR4 (yCCR4), which was originally identified as a gene that affects nonfermentative gene expression, is involved in both positive and negative regulation of transcription through its interactions with transcription factors (16). Recent biochemical studies revealed that yCCR4 belongs to the exonuclease III family and displays 3′-5′ poly(A) exoribonuclease activity in vitro. The rate of mRNA deadenylation is reduced in deletion mutants of yCCR4 (6, 31). Intriguingly, yCCR4 deletion mutants show gross abnormalities, such as growth defects, on glucose-depleted medium and increased sensitivities to hydroxyurea, ionizing radiation, and X rays (8, 19, 30, 33). In addition, decreased expression of CCR4 in *Drosophila melanogaster* causes female sterility (17, 29) and embryonic lethality by increasing the poly(A) tail length (PAT) of *nanos* mRNA (37). These data suggest that the deadenylase activity of CCR4 contributes to cellular homeostasis. However, the molecular characteristics and biological functions of mammalian CCR4 remain unclear.

In mammals, there are two genes homologous to yeast *CCR4*, *CCR4a*/*CNOT6* and the newly identified *CCR4b*/*CNOT6L*. In the present study, we show that CCR4b displays deadenylase activity in vitro and in vivo. CCR4b associates, like CCR4a, with human CNOT1, CNOT2, CNOT3, CAF1a/

* Corresponding author. Mailing address: Division of Oncology, Department of Cancer Biology, Institute of Medical Science, University of Tokyo, Tokyo 108-8639, Japan. Phone: 81 3 5449 5301. Fax: 81 3 5449 5413. E-mail: tyamamot@ims.u-tokyo.ac.jp.

▽ Published ahead of print on 23 April 2007.

CNOT7, CAF1b/CNOT8, and CAF40/CNOT9, forming a multisubunit complex. We also show that the deadenylase activity of CCR4b is associated with cell proliferation and regulates cellular levels of $p27^{Kip1}$ mRNA and protein. Our findings provide evidence that CCR4b-associated deadenylase activity plays a significant role in cell proliferation.

MATERIALS AND METHODS

Plasmids, cell culture, and expression. The human CCR4b cDNA was cloned by reverse transcription-PCR from total RNAs of HEK293T human embryonic kidney cells. The deadenylase-negative CCR4b and the RNA interference (RNAi)-refractory CCR4b were generated by PCR-based mutagenesis. For preparation of glutathione *S*-transferase (GST) fusion proteins, the CCR4b cDNA fragment encoding amino acids 157 to 402 was cloned in frame into the pGEX 6P-1 plasmid (Amersham Biosciences). Full-length cDNA encoding wild-type or deadenylase-negative mutant CCR4b was inserted either into the pME18S mammalian expression vector as a GST fusion form or into pEGFP-C1 (Clontech) or a retrovirus vector, pMXs-neo. To construct the short hairpin RNA (shRNA) expression vector, synthetic two-oligonucleotide primers were annealed and then introduced into the pSIREN-RetroQ vector according to the manufacturer's protocol (BD Biosciences). The oligonucleotide sequence consisted of a 19-nt sequence (GCCTGATGCCTTACACCAA, nt 1424 to 1442 of mouse *CCR4a*, and GACCCAGAGTATTCTGATG, nt 1075 to 1093 of mouse *CCR4b*). RNAi-refractory CCR4b contained three silent mutations (lowercase) within the siRNA target sequence (GACCCtGAGTAcTCcGATG). A control vector was constructed with a 19-nt sequence (TTCTCCGAACGTGTCACGT) with no significant homology to any mammalian gene sequence to serve as a nonsilencing control. For promoter activity analysis, p27-PF and p27-ApaI, promoter regions of the $p27^{Kip1}$ gene, were inserted upstream of the luciferase gene (13). For UTR luciferase assays, the 5′ UTR and 3′ UTR of $p27^{Kip1}$ mRNA were inserted upstream and downstream of the luciferase coding region to produce 5′ UTR-plus-Luc and Luc-plus-3′ UTR constructs, respectively (11). pRL-TK was used as a control. HEK293T cells and NIH 3T3 cells were cultured and transfected with plasmids as described previously (21, 28). Retroviral infection of NIH 3T3 cells was performed as described previously (28). For promoter activity analysis and UTR luciferase assays, NIH 3T3 cells were transfected with the plasmids with FuGENE6 Transfection Reagent (Roche), and 48 h after transfection, the cell extracts were analyzed for luciferase activity with a Dual-Luciferase Reporter System (Promega).

Northern blot and Southern blot analyses. Total RNAs were isolated with ISOGEN according to the manufacturer's protocol (Nippon Gene). Northern blot and Southern blot analyses were carried out as described previously (36). To prepare the probes, DNA fragments of human *CCR4a* (nt 1 to 500), human *CCR4b* (nt 1 to 500), human β-*actin* (nt 1 to 1800), mouse $p21^{Cip1}$ (3′ UTR; nt 1601 to 1900), mouse $p27^{Kip1}$ (3′ UTR; nt 2771 to 3070), and mouse *GAPDH* (glyceraldehyde-3-phosphate dehydrogenase) (3′UTR; nt 921 to 1220) were amplified by PCR. The probes were labeled with [α-^{32}P]dCTP by a random-prime labeling system as described previously (21) and were hybridized to home-made blots or multiple-human-tissue Northern blots at 65°C for 2 h in ExpressHyb Hybridization Solution (Clontech).

Antibodies. Polyclonal antibodies against CCR4b, CNOT3, and CNOT9 were raised by immunizing rabbits with recombinant human CCR4b (amino acids 152 to 401), CNOT3 (amino acids 1 to 753), and CNOT9 (amino acids 1 to 299), respectively. The recombinant proteins were produced in *Escherichia coli* as GST fusion proteins. Anti-RB antibody (C-15), anti-cyclin D1 antibody (72-13G), anti-cyclin A antibody (H-432), anti-p21^{Cip1} antibody (F-5), anti-cdk2 antibody (M-2), anti-cdk4 antibody (C-22), and anti-GST antibody (B-14) were purchased from Santa Cruz Biotechnology. Anti-Flag antibody (M2), anti-GFP antibody (598), and anti-p27^{Kip1} antibody (06-445) were from Sigma, MBL, and UBI, respectively.

Immunobiochemistry and immunocytochemistry. Preparation of cell lysates, immunoprecipitation, and immunoblotting were carried out as described previously (21, 28). Immunofluorescence analysis of the cells and cell fractionation were carried out as described previously (14).

Mass analysis. HEK293T cells were transfected with either GFP-tagged CCR4a/b or GFP-only expression plasmids. Forty-eight hours after transfection, total cell lysates (20 mg) were prepared from the cells and immunoprecipitated with the anti-GFP antibody. Immunoprecipitates were washed successively five times with lysis buffer (1% NP-40, 50 mM Tris-HCl [pH 7.5], 150 mM NaCl, 1 mM EDTA, 1 mM phenylmethylsulfonyl fluoride, 1 mM NaF, 1 mM Na_3VO_4). The components of the immunoprecipitated complexes were fractionated by 10% sodium dodecyl sulfate-polyacrylamide gel electrophoresis (SDS-PAGE) and visualized by Coomassie brilliant blue staining or SilverQuest (Invitrogen). Specific bands were excised from the gel and digested with trypsin. A small aliquot of the peptide mixture from in-gel digestion of the bands was analyzed by matrix-assisted laser desorption–ionization. High-resolution peptide mass maps were analyzed by Mascot (Matrix Science) search.

Nuclease assay. HEK293T cells were transfected with GST-CCR4b expression plasmids. Forty-eight hours after transfection, lysates were prepared from the cells and subjected to coprecipitation experiments. The GST-CCR4b precipitates in nuclease buffer (50 mM HEPES-NaOH, 150 mM NaCl, 2 mM $MgCl_2$, 10% glycerol, 1 mM dithiothreitol, pH 7.4) were incubated at 37°C for 60 min, together with synthesized RNA substrate (5′-UCUAAAUAAAAAAAAAAAA AAAAAAA-3′; final concentration, 0.1 μM) labeled with fluorescein isothiocyanate at the 5′ end. The reaction mixtures were fractionated on a 7 M urea-25% sequence polyacrylamide denaturing gel. The products were analyzed and quantified with a fluorescence imager, FLA-5000 (FUJIFILM).

Cell growth analysis. NIH 3T3 cells (5×10^4) infected with shRNA-harboring viruses were plated in 6-cm dishes. At 1, 2, 3, and 4 days after being seeded, the living cells were counted. For colony formation assays, cells (1×10^3) were plated in 6-cm dishes and stained with Giemsa's solution after 2 weeks. For flow cytometry, cells were fixed with 100% cold ethanol and then stained with propidium iodide (50 μg/ml). The percentages of cells in the G_0/G_1, S, and G_2/M phases of the cell cycle were determined by FACSCalibur (BD Biosciences).

Assays of mRNA stability. Cells were treated with actinomycin D (2.5 μg/ml), and total RNA was extracted at the indicated time points and analyzed by Northern blotting. The level of $p27^{Kip1}$ mRNA on Northern blots was normalized to that of *GAPDH* mRNA.

PAT assay. The PAT assay was carried out according to the method of Salles et al. (25) with some minor modifications. In brief, 0.1 μg of total RNA was used for reverse transcription with an anchoring nucleotide-fused oligo(dT)$_{12}$ primer (5′-AATGCCAGCTCCGCGGCCGCGTTTTTTTTTTT-3′). PCR was performed with an anchoring sequence (5′-GCCAGCTCCGCGGCCGCG-3′) and a sense primer targeting a specific sequence in the cDNA of interest ($p27^{Kip1}$, 5′-ACTCTGATGTGTTATGGTTCCTGAATTTCT; $p21^{Cip1}$, 5′-TCTTGGGG GCTAAGGGAGCTCACAGGACAC). The PCR products were resolved on 2% agarose gels and visualized by Southern blot analysis.

Microarray analysis. Total RNAs were extracted from control or CCR4b-depleted cells. Following the isolation of RNA, all subsequent technical procedures, including quality control of RNA, labeling, hybridization, and scanning of the arrays, were performed in BIO MATRIX Research, Inc., cDNA, and biotin-labeled cRNA was synthesized according to protocols for Affymetrix array analysis. Biotin-labeled cRNAs (15 μg) were hybridized to the GeneChip Mouse Genome 430 2.0 Array (Affymetrix, Santa Clara, CA). To determine the average differences for each probe set, changes were calculated by a global normalization method using Affymetrix GCOS (GeneChipOperating Software) software. Changes in the expression of a particular gene were a 2.0-fold change or greater and more than 100 in raw data for inclusion in Table 1.

RESULTS

cDNA cloning and tissue distribution of a new CCR4 family member, CCR4b. To investigate the function of CCR4 in mammals, we searched the NCBI database (BLAST searches) for a mammalian counterpart of yeast *CCR4* and identified two cDNA clones, human KIAA1194 (6.2 kbp) and human NM_144571 (8.8 kbp), that share significant homology with yeast *CCR4*. The genes for these cDNAs have been identified and named *CCR4a* and *CCR4b*, respectively (35). We have determined the nucleotide sequences of the human and murine *CCR4b* cDNAs, and the deduced amino acid sequences were compared and aligned with the known sequences of *Saccharomyces cerevisiae* and *D. melanogaster* CCR4 (Fig. 1A). The human and mouse CCR4b sequences showed 98% identity, the human and mouse CCR4a sequences showed 96% identity, and human CCR4b and human CCR4a showed 78% identity. Moreover, human CCR4b showed significant homology with fly CCR4 (59% identity) and with yeast CCR4 (33%

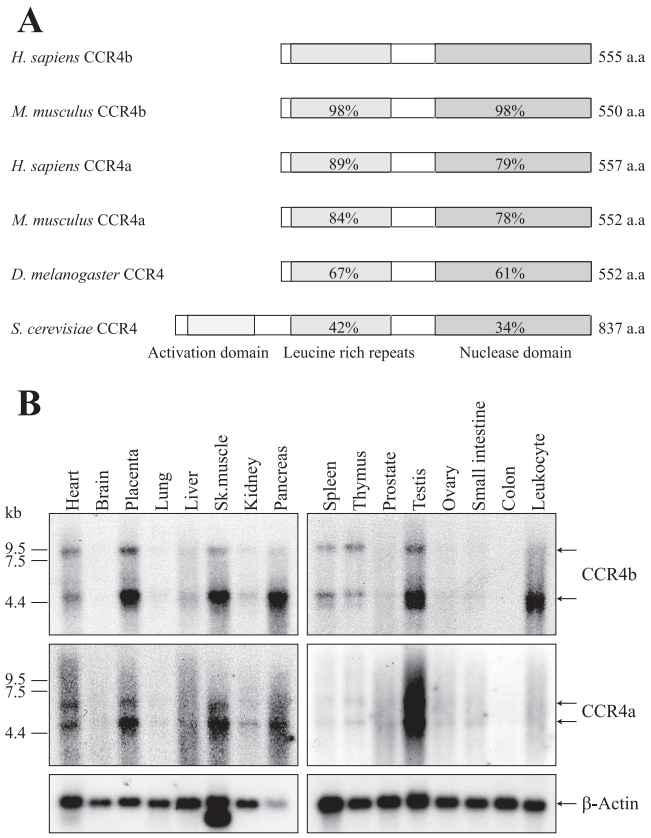

FIG. 1. Sequence alignment and tissue distribution of CCR4 family proteins. (A) Schematic representation of conserved regions shared among CCR4a and CCR4b from *Homo sapiens* and *Mus musculus* and CCR4 from *D. melanogaster* and *S. cerevisiae*. The percentages of amino acid identity for the leucine-rich repeat domain and the nuclease catalytic domain are indicated. a.a, amino acids. (B) Expression of *CCR4a* and *CCR4b* mRNAs in human tissues. A multiple-human-tissue Northern blot was hybridized with probes specific for *CCR4a* and *CCR4b*. A β-*actin*-specific probe was used as an internal control for RNA loading.

identity), indicating high sequence conservation during evolution.

We then examined the expression of *CCR4a* and *CCR4b* in human tissues by Northern blot hybridization (Fig. 1B). We detected multiple bands with CCR4a and CCR4b probes. By searching the NCBI database for expressed cDNA, we found that CCR4a and CCR4b each have two splicing variants, which might explain the occurrence of multiple bands in the Northern blot. Expression of both *CCR4a* and *CCR4b* mRNAs was observed in several tissues. The high levels of expression of these mRNAs were seen in placenta, skeletal muscle, pancreas, and testis.

Identification of CCR4a/b-associated proteins. To characterize the human CCR4 homolog further, we transfected HEK293T cells with vector expressing GFP-tagged CCR4a, CCR4b, or CCR4b with the E239A mutation. CCR4a- or CCR4b-containing protein complexes were prepared from the cell lysates by coimmunoprecipitation with anti-GFP antibody. Separation of the immunoprecipitates by SDS-PAGE revealed a number of proteins that interacted with CCR4a or CCR4b (Fig. 2A). Control immunoprecipitation from lysates of GFP-transfected HEK293T cells yielded no specific interacting proteins (Fig. 2A, lane 1). Mass spectrometry of the anti-GFP-CCR4b immunoprecipitates identified CNOT1, CNOT2, CNOT3, CAF1b/CNOT8, and CAF40/CNOT9, as well as the putative proteins encoded by KIAA1741 and AAH02928 cDNAs, as its interacting proteins (Fig. 2A, lane 2). CNOT1, CNOT2, CNOT3, CAF1b/CNOT8, and CAF40/CNOT9 are human homologs of the components of the yeast CCR4-NOT complex. KIAA1741 and AAH02928 are found only in higher eukaryotes. KIAA1741 encodes a 182-kDa tankyrase 1-binding protein (26), and AAH02928 is a tetratricopeptide repeat domain-containing protein that appears to contribute to protein-protein interactions. These proteins had been little characterized. Virtually identical results were obtained with lysates from GFP-CCR4a-expressing HEK293T cells (Fig. 2A, lane 4). Although the glutamic acid at amino acid position 239 is necessary for the magnesium ion binding that is required for deadenylase activity, replacement of this amino acid with alanine did not grossly affect the association of CCR4b with other proteins (Fig. 2A, lane 3). In the gels, other specific bands were seen, whose identification by mass spectrometric analysis was not successful. From these bands, we could identify many peptide sequences of unknown origin but not specific proteins by MASCOT analysis. This was probably due at least in part to the existence of multiple proteins in each of these bands or to some unknown technical problems. The above-mentioned data indicated that mammalian CCR4a and CCR4b form multisubunit complexes similar to the yeast CCR4-NOT complex. In the following experiments, we focused our studies on characterization of CCR4b.

To confirm the interactions of CCR4b with some of the proteins identified above and with well-known CCR4-associated CAF1a/CNOT7, we performed coimmunoprecipitation experiments. Vector expressing GFP-tagged CCR4b was transfected into HEK293T cells, together with a Flag-tagged expression vector encoding Flag-tagged CNOT3, CAF1a, or CAF1b. Lysates of transfectants were subjected to anti-Flag immunoprecipitation, followed by immunoblotting with anti-GFP antibody (Fig. 2B). These proteins were all coimmunoprecipitated with GFP-CCR4b. We then examined by coimmunoprecipitation experiments whether the interactions occurred between the endogenous proteins. Lysates from NIH 3T3 cells were subjected to anti-CCR4b immunoprecipitation, followed by immunoblotting with anti-CNOT1, anti-CNOT3, anti-CAF1a, and anti-CAF40 antibodies (Fig. 2C). CNOT1, CNOT3, CAF1a, and CAF40 were all coimmunoprecipitated with CCR4b, substantiating the presence of a CCR4-NOT complex in mammals.

Subcellular localization of CCR4b. Previous reports indicated that yeast CCR4 is involved in two cellular functions, transcriptional regulation in the nucleus and deadenylation of mRNAs in the cytoplasm (8, 9). To assess the possible function of mammalian CCR4b, we examined the subcellular localization of CCR4b protein in NIH 3T3 cells transfected with expression plasmid encoding GFP-CCR4b. Immunofluorescence analysis revealed that GFP-CCR4b was present predominantly in the cytoplasm (Fig. 3A). Similar results were obtained when NIH 3T3 cells were infected with nontagged CCR4b expression vector, followed by immunostaining with anti-CCR4b antibodies (Fig. 3B).

To confirm the above-mentioned results, we performed sub-

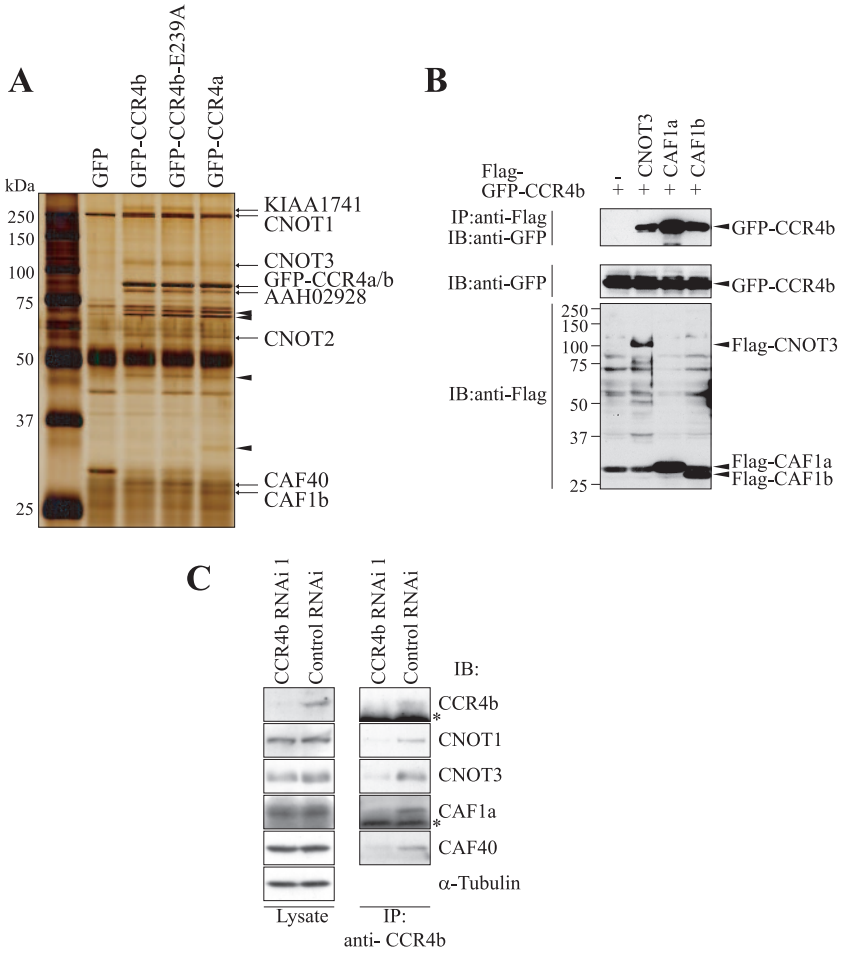

FIG. 2. Identification of proteins that interact with CCR4a and CCR4b. (A) Purification and identification of polypeptides associated with CCR4a and CCR4b. Cytoplasmic extracts from HEK293T cells expressing green fluorescent protein (GFP)-tagged CCR4a, CCR4b, or CCR4b with an E239A mutation were immunoprecipitated with GFP antibody. Immunoprecipitates were separated by 10% SDS-PAGE, and the associated polypeptides were visualized by silver staining. The arrows and arrowheads indicate identified proteins and unidentified proteins, respectively. (B) Interaction between CCR4b and other components of the CCR4-NOT complex in HEK293T cells. HEK293T cells were transfected with the plasmid coding for GFP-tagged CCR4b, together with the plasmid for CNOT3, CAF1a, or CAF1b, which were all tagged with Flag. Cell lysates were prepared 48 h after transfection. Interactions were examined by immunoprecipitation (IP) with anti-Flag antibody, followed by immunoblotting (IB) with anti-GFP antibody (top). Expression of GFP-tagged CCR4b and Flag-tagged proteins is shown in the middle and bottom, respectively. (C) Endogenous interactions between CCR4b and CNOT1, CNOT3, CNOT7, and CNOT9. NIH 3T3 cell lysates were subjected to immunoprecipitation with anti-CCR4b antibody, followed by immunoblotting with anti-CNOT1, CNOT3, CNOT7, and CNOT9 antibodies. Lysates and immunoprecipitation are shown on the left and right, respectively. The asterisks indicate immunoglobulin G heavy chain (CNOT6L) and light chain (CNOT7).

cellular fractionation of NIH 3T3 cells, and each fraction was subjected to immunoblotting with anti-CCR4b antibodies. The efficacy of fractionation was monitored by nuclear CBP and cytoplasmic Raf-1. Consistent with the results shown above, endogenous CCR4b was detected mainly in the cytoplasmic fraction (Fig. 3C).

CCR4b displays 3′-5′ poly(A) exoribonuclease activity. yCCR4 is a catalytic component of the cytoplasmic deadenylase complex, and its C-terminal region is highly homologous to apurinic endonucleases (6). Putative catalytic residues present in the C-terminal region of yCCR4 were conserved in CCR4a and CCR4b. We examined whether CCR4b was associated with deadenylase activity by an in vitro deadenylase assay with single-stranded poly(A) RNA as a substrate. Vector expressing GST-tagged CCR4b was transfected into HEK293T cells, and the GST-tagged protein was purified with glutathione-Sepharose beads. We then incubated the purified proteins with a poly(A) RNA substrate. Analysis of the reaction products on the denaturing sequencing gel revealed cleavage of the poly(A) RNA substrate (Fig. 4A and B). Because the substrate was 5′-end labeled, the generation of an RNA ladder indicated trimming of the substrate from the 3′ end, suggesting that CCR4b had deadenylase activity in vitro (Fig. 4A and C). Five residues, Glu195, Glu239, Asp410, Asp489, and His529 of CCR4b, were aligned with the active-site residues of nuclease/phosphatase family proteins (6). We introduced the Glu195Ala (E195A), Glu239Ala (E239A), Asp410Ala (D410A), Asp489Ala (D489A), or His529Ala (H529A) substitution into CCR4b. These mutant proteins were expressed in HEK293T cells and purified with glutathione-Sepharose, and their deadenylase activities were evaluated as shown in Fig. 4A. We

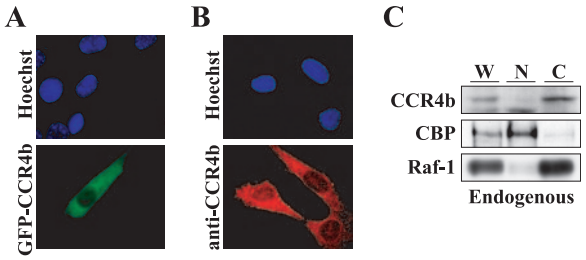

FIG. 3. Subcellular localization of CCR4b in NIH 3T3 cells. (A) NIH 3T3 cells were transfected with vector expressing GFP-CCR4b and fixed 24 h after transfection. Expression of GFP-CCR4b (green) was examined by fluorescence microscopy. (B) NIH 3T3 cells were infected with retrovirus expressing CCR4b and stained with anti-CCR4b antibodies (red). Nuclei were stained with Hoechst 33342 (blue) (top in A and B). (C) Subcellular localization of the endogenous CCR4b protein. Proteins from NIH 3T3 cells were subfractionated, and each fraction was subjected to immunoblotting with anti-CCR4b, anti-CBP (marker of the nuclear fraction), and anti-Raf-1 (a marker of the cytoplasmic fraction). W, whole-cell lysates; N, nuclear fraction; C, cytoplasmic fraction.

found that none of the mutated forms of CCR4b had deadenylase activity, confirming that each of the five conserved residues is critical for deadenylase activity (Fig. 4C).

Suppression of CCR4b, but not CCR4a, impairs the growth of NIH 3T3 cells. To clarify the biological significance of CCR4a and CCR4b, we generated a retrovirus-based vector expressing CCR4a and CCR4b shRNAs under the control of the U6 promoter. The retroviral vector also expressed the puromycin phosphotransferase gene, which allowed selection of transduced cells with puromycin. After NIH 3T3 cells were infected with the viruses, lysates of retrovirus-infected and puromycin-selected cells were prepared and then subjected to Northern blot analysis. As shown in Fig. 5A, *CCR4a* and *CCR4b* mRNA expression was almost completely inhibited by CCR4a- and CCR4b-specific shRNA. We found that although the proliferation rate of CCR4b-depleted cells was significantly lower than that of control shRNA-treated cells (Fig. 5B), depletion of CCR4a had little effect on cell proliferation (data not shown). Severe reduction of proliferation of CCR4b-depleted cells was also observed in colony formation experiments (Fig. 5C). Flow cytometric analysis showed that the proportion of G_0/G_1 phase cells (83%) was elevated and that of S phase cells (5%) was reduced by CCR4b depletion in comparison with control cells (G_0/G_1, 57%; S, 16%) (Fig. 5D). These data suggested that CCR4b depletion inhibited progression of the cell cycle from G_0/G_1 to S phase.

Alteration of cell cycle-related gene expression in CCR4b-depleted cells. A series of cyclin and cyclin-dependent kinases (CDKs) plays a central role in cell cycle progression (for a review, see reference 27). The levels of cyclins oscillate during the cell cycle, and CDK activities depend on the cyclin expression levels. In mammalian cells, the cyclin D-CDK4 and cyclin E-CDK2 complexes regulate G_1/S progression. The retinoblastoma (RB) protein is one of their substrates, and phosphorylation of RB leads to G_1/S progression. The activities of these cyclin-CDK complexes are inhibited by CDK inhibitors, such as $p27^{Kip1}$ and $p21^{Cip1}$, which mediate G_0/G_1 arrest. To investigate the molecular mechanism that underlies G_0/G_1 arrest in CCR4b-depleted cells, we examined the expression of cell cycle-related proteins, including cyclins, CDKs, and CDK inhibitors, by immunoblotting (Fig. 5E). We found that expression of $p27^{Kip1}$ was increased significantly by CCR4b depletion, whereas expression of $p21^{Cip1}$, CDK2, and CDK4 in the CCR4b-depleted cells was similar to that in control cells. Levels of cyclin D1 and cyclin A were decreased in CCR4b-depleted cells. Consistent with these results, the unphosphorylated form of RB became dominant in CCR4b-depleted cells (Fig. 5F). Thus, increased expression of $p27^{Kip1}$ in CCR4b-depleted cells would contribute to G_0/G_1 arrest of the cell cycle progression. Significant cleavage of poly(ADP-ribose) polymerase was not observed, suggesting that CCR4b depletion-mediated growth suppression was not related to apoptotic cell death.

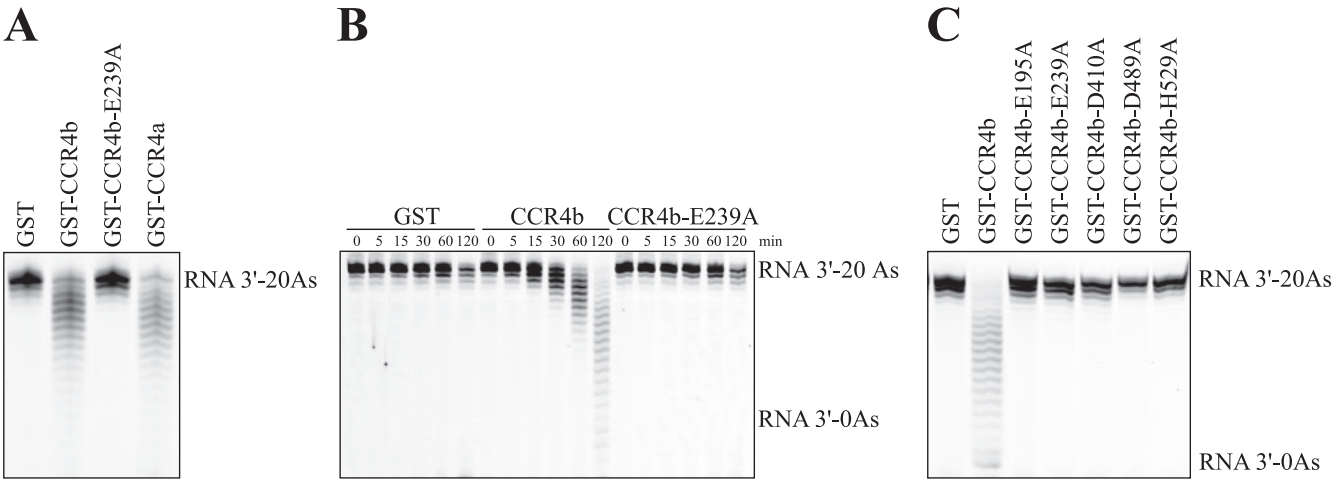

FIG. 4. Deadenylase activity of CCR4b in vitro. (A) GST-CCR4a and GST-CCR4b proteins were expressed in HEK293T cells and precipitated with glutathione-Sepharose. 5′-fluorescein isothiocyanate-labeled RNA substrate (RNA 3′-20 As) was incubated with each GST fusion protein for 60 min. The labeled RNA was then analyzed on a denaturing sequencing gel. (B) Time course of GST-CCR4b enzymatic activity. The reaction was performed as described for panel A, except for the incubation time. The indicated times refer to the minutes of incubation prior to termination of the enzymatic reaction. (C) Enzymatic activities of five CCR4b mutations were tested as described for panel A.

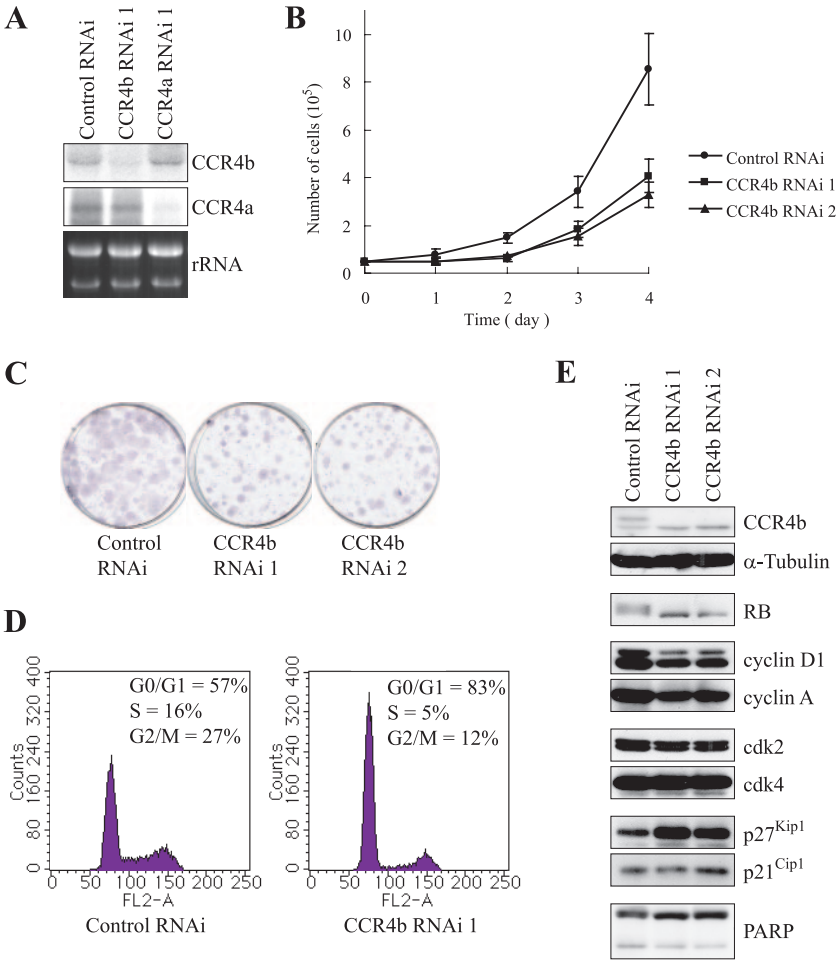

FIG. 5. CCR4b, but not CCR4a, RNAi inhibits the growth of NIH 3T3 cells. (A) Northern blot analysis showing expression of endogenous CCR4a and CCR4b transcripts in NIH 3T3 cells. The identity of each transcript was confirmed by RNAi knockdown experiments. (B) NIH 3T3 cells (5×10^4) infected with a retrovirus expressing CCR4a and CCR4b shRNAs were seeded in 6-cm dishes, and cell numbers were determined at the indicated time points. Each data point is the mean of three independent experiments. The error bars represent standard deviations. (C) Control and CCR4b RNAi cells (1×10^3) were plated in 6-cm dishes, and colonies were stained with Giemsa's solution after 2 weeks. (D) The DNA contents of control and CCR4b-depleted cells were determined by fluorescence-activated cell sorting. The percentages of cells in the G_0/G_1, S, and G_2/M phases of the cell cycle were quantified. (E) Expression levels of cell cycle regulatory proteins were examined by Western blotting. The proteins were identified and quantified with anti-CCR4b, anti-α-tubulin, anti-RB, anti-cyclin A, anti-cyclin D1, anti-cdk2, anti-cdk4, anti-$p27^{Kip1}$, anti-$p21^{Cip1}$, and anti-poly(ADP-ribose) polymerase (PARP) antibodies. Detection of α-tubulin was performed as an internal control for protein loading.

Deadenylase activity of CCR4b is essential for regulation of cell growth. To examine the significance of the CCR4b deadenylase activity in normal cell growth, we prepared retrovirus vectors expressing RNAi-refractory wild-type CCR4b (rCCR4b-WT) and mutant CCR4b (rCCR4b-E239A) that has no deadenylase activity in vitro (Fig. 4B). The expression levels of rCCR4b-WT and rCCR4b-E239A were similar in immunoblotting experiments (Fig. 6B). Ectopic expression of rCCR4b restored the proliferation of CCR4b-depleted cells (Fig. 6A), confirming that the growth defect was not due to off-target effects by CCR4b shRNA. Importantly, ectopic expression of rCCR4b-E239A did not rescue the growth defect caused by CCR4b depletion (Fig. 6A). The profile of expression of cell cycle-related genes in rCCR4b-expressing cells was similar to that in control cells (Fig. 6B, lanes 1 and 3). On the other hand, in the rCCR4b-E239A-expressing cells, $p27^{Kip1}$ and cyclin D1 expression and the phosphorylation state of RB protein did not return to a level similar to that in control cells (Fig. 6B, lanes 1 and 4). These data suggested that the deadenylase activity of CCR4b played an important part in cell growth regulation.

Stability of *$p27^{Kip1}$* mRNA is increased in CCR4b-depleted cells. Given that the deadenylase activity of CCR4b influences the stability of mRNAs, levels of CCR4b target mRNAs would be increased in CCR4b-depleted cells. We compared the expression profiles of the cellular genes between control and CCR4b-depleted NIH 3T3 cells by DNA microarray analysis (Fig. 7). Among 1,508 cell cycle-related genes described in the analysis, the level of *$p27^{Kip1}$* mRNA was prominently increased in CCR4b-depleted cells (Table 1). There were other genes whose expression might be increased, but the significance was low. We further confirmed by Northern blot analysis that the *$p27^{Kip1}$* mRNA level was

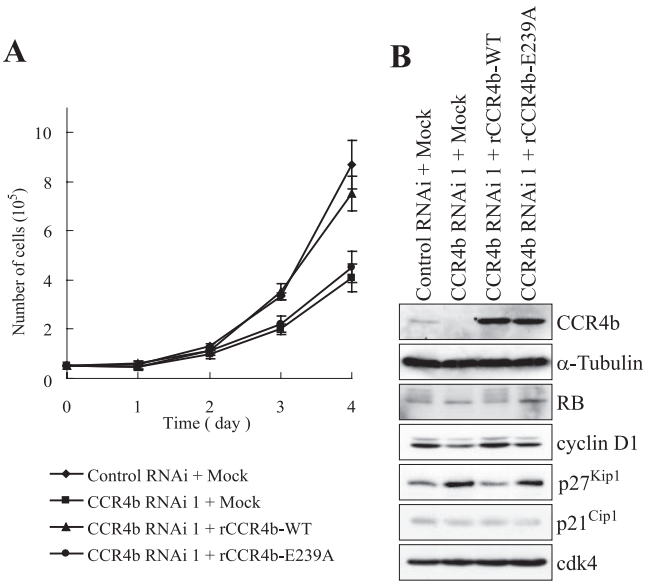

FIG. 6. Deadenylase activity of CCR4b is essential for growth of NIH 3T3 cells. (A) Growth of CCR4b-depleted NIH 3T3 cells infected with vector expressing wild-type or a nuclease mutant of CCR4b was examined as described in the legend to Fig. 5A. (B) Expression of cell cycle regulatory proteins in NIH 3T3 cells was analyzed by Western blotting as in Fig. 5D. Protein levels were identified with anti-CCR4b, anti-α-tubulin, anti-RB, anti-cyclin D1, anti-$p27^{Kip1}$, and anti-$p21^{Cip1}$ antibodies. Detection of α-tubulin was performed as an internal control for protein loading.

increased in the absence of CCR4b, whereas the $p21^{Cip1}$ mRNA level was not affected (Fig. 8A).

We next examined the half-life of $p27^{Kip1}$ mRNA. Control and CCR4b-depleted NIH 3T3 cells were treated with actinomycin D to inhibit de novo transcription. The amounts of $p27^{Kip1}$ mRNA at various time points after actinomycin D treatment were analyzed. We found that the rate of decline in $p27^{Kip1}$ transcript levels was lower in CCR4b-depleted cells than in control cells (Fig. 8C). The half-lives of $p27^{Kip1}$ mRNA were 1.8 h and 1.3 h in CCR4b-depleted and control cells, respectively (Fig. 8D). To rule out the possibility that the $p27^{Kip1}$ mRNA level was increased by transcriptional activation, we examined the promoter activity of the $p27^{Kip1}$ gene. We transfected control or CCR4b-depleted NIH 3T3 cells with luciferase constructs that contained the human $p27^{Kip1}$ promoter (p27-PF, nt −3568 to −12, and p27-ApaI, nt −774 to −12) (13). Because the transcriptional activities of these reporter constructs are activated by vitamin D_3 and transcription factor NF-Y, which are known to affect transcription of the endogenous $p27^{Kip1}$ gene, they likely mimic the endogenous promoter, at least to a certain extent. The luciferase activity in the lysates of CCR4b-depleted cells was not significantly different from that of control cells (Fig. 8B). These data suggested that the increase in the levels of $p27^{Kip1}$ mRNA was the result of its enhanced stability.

Mechanism of CCR4b action. To investigate the mechanism by which $p27^{Kip1}$ mRNA stability is affected by CCR4b deadenylase, we performed UTR luciferase assays. The 5′ UTR and 3′ UTR of $p27^{Kip1}$ mRNA were inserted upstream and down-

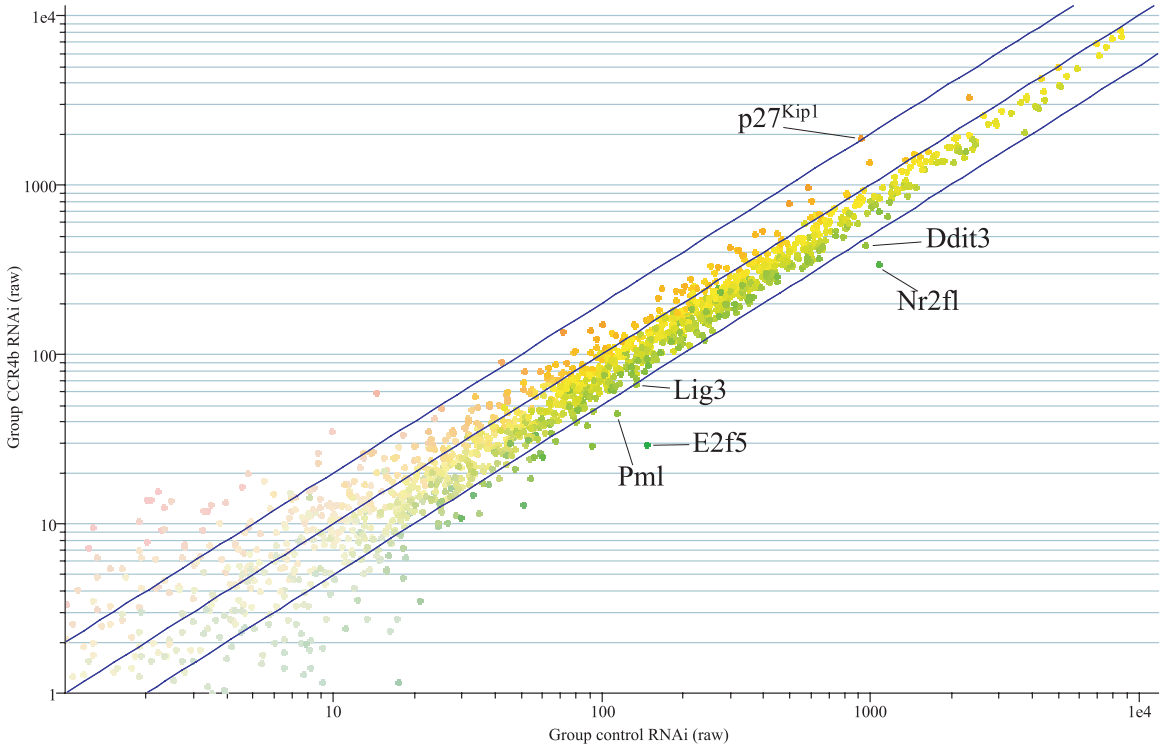

FIG. 7. Scatter plot analysis of average differences in mRNA populations isolated from control and CCR4b-depleted cells. Listed on the *x* and *y* axes are the log-transformed intensity data. The diagonal lines show the linear repression of the intensity data, the solid lines represent the same, and the thin lines represent the 2.0-fold change between control and CCR4b-depleted cells.

TABLE 1. Genes expressed differentially between control and CCR4b RNAi cells

No.	Accession no.	Gene	Molecular characteristics	Raw data		
				Control	CCR4b	Change (*n*-fold)
Increased in CCR4b-depleted cells						
1	NM_009875	p27Kip1	Protein kinase inhibitor activity	913.1	1,893.0	2.1
Decreased in CCR4b-depleted cells						
2	NM_010151	Nr2f1	Nuclear receptor	1,070.0	339.6	−3.2
3	NM_007837	Ddit3	Transcription	957.4	445.1	−2.2
4	BB286270	E2f5	Transcription	145.2	29.5	−4.9
5	C80352	Lig3	DNA replication	133.1	66.7	−2.0
6	BB667149	Pm1	Transcription	112.8	44.7	−2.5

stream of the luciferase coding region, respectively (11). We transfected control or CCR4b-depleted NIH 3T3 cells with luciferase constructs (control Luc, 5′ UTR plus Luc, and Luc plus 3′ UTR) and determined the luciferase activities in cell lysates. The results showed that the luciferase activity of 5′ UTR plus Luc was not significantly affected by the presence or absence of CCR4b (Fig. 9A, middle). In contrast, the luciferase activity of Luc plus 3′ UTR was decreased more than that of Luc only in the control cells (Fig. 9A, right). This result was most likely due to ARE sequences of $p27^{Kip1}$ mRNA, which would promote rapid deadenylation-dependent mRNA degradation (11, 24). Importantly, in the CCR4b-depleted cells, the luciferase activities of Luc plus 3′ UTR was not decreased (Fig. 9A, right). These data suggested that CCR4b contributes to the deadenylation and degradation of $p27^{Kip1}$ mRNA through the 3′ UTR ARE-mediated mechanism in vivo.

To demonstrate that CCR4b depletion inhibits the shortening of the poly(A) tail of $p27^{Kip1}$ mRNA, we performed PAT assays (25). In CCR4b-depleted cells, the poly(A) tail of $p27^{Kip1}$ mRNA, but not that of $p21^{Cip1}$ mRNA, was significantly longer than that in control cells (Fig. 9B). These data suggested that CCR4b functions as a deadenylase for the poly(A) tail of $p27^{Kip1}$ mRNA in vivo.

DISCUSSION

There is accumulating evidence that the CCR4-NOT complex is involved in the control of gene expression at either the transcription level or the mRNA deadenylation level or both (8, 9). For example, CNOT proteins are components of the CCR4-NOT transcriptional complex that affect, both positively and negatively, the transcription of genes involved in the fermentative growth, cell wall integrity, and ion sensitivity of yeast (16). We reported previously that CAF1a/CNOT7 interacts with nuclear receptor RXRβ and stimulates retinoic acid-dependent activation of RXRβ-driven transcription (20). Other reports have shown that the CCR4-NOT complex is involved in deadenylation (6, 31). yCCR4 belongs to the exonuclease III family and displays deadenylase activity in vitro. The rate of mRNA deadenylation is reduced in the absence of CCR4. In the present study, we found that mammalian CCR4a/b have deadenylase activity in vitro. CCR4b regulates the growth of NIH 3T3 cells in a manner dependent on deadenylase activity. $p27^{Kip1}$ mRNA is stabilized in CCR4b-depleted cells, indicating that $p27^{Kip1}$ transcript is a target of CCR4b deadenylase. Our study provides the first evidence that CCR4b deadenylase regulates the stability of an mRNA associated with cell cycle progression and influences the growth of mammalian cells.

Mammalian CCR4a and CCR4b show exoribonuclease activities in vitro (Fig. 4) and form a multisubunit complex similar to the yeast CCR4-NOT complex (Fig. 2). CCR4a and CCR4b are expressed similarly in NIH 3T3 cells. Although depletion of CCR4b causes the growth defect, depletion of CCR4a has little effect on cell proliferation. This suggests that CCR4a and CCR4b might play different roles and have different target mRNAs. The CCR4-NOT complex in yeast includes another nuclease, CAF1. Both yeast CAF1 and mouse CAF1a display deadenylase activity in vitro and in vivo (32). In the present study, we showed that a CCR4b mutant lacking deadenylase activity forms a multisubunit complex that includes CAF1a/b (Fig. 2A), but it cannot restore proliferation of CCR4b-depleted cells (Fig. 6). This suggests that the specific function of CCR4b is not replaced by either CAF1a or CAF1b deadenylase. Another group also showed that mouse CAF1a deadenylase activity is not relevant to in vivo function (32). It was previously reported that yeast CAF1 is required for the interaction of CCR4 with other components of the CCR4-NOT complex (7). These results suggest that CCR4b is the principal deadenylase in the CCR4-NOT complex. Although the precise functions of the other components of the CCR4-NOT complex are unclear, there is evidence that these proteins regulate CCR4-mediated deadenylation. Deletion analysis of the yeast *NOT* genes revealed a defect in the deadenylation rates of several target mRNAs (6, 18, 31). In addition, NOT4 has an RNA recognition motif, suggesting that CNOT4 might be involved in the recognition of target mRNAs (8).

CCR4b has an exonuclease domain in its primary structure (Fig. 1A). We showed that CCR4b indeed has an in vitro deadenylase activity for synthetic poly(A) RNA substrate (Fig. 4). We then showed that, in the CCR4b-depleted cells, the poly(A) tail of $p27^{Kip1}$ mRNA is significantly longer than that in control cells (Fig. 9B). Furthermore, by examining the effect of CCR4b on the 3′ UTR of $p27^{Kip1}$ mRNA, we obtained data suggesting that CCR4b may destabilize a chimeric luciferase mRNA ligated to the 3′ UTR of $p27^{Kip1}$ mRNA (Fig. 9A). It is

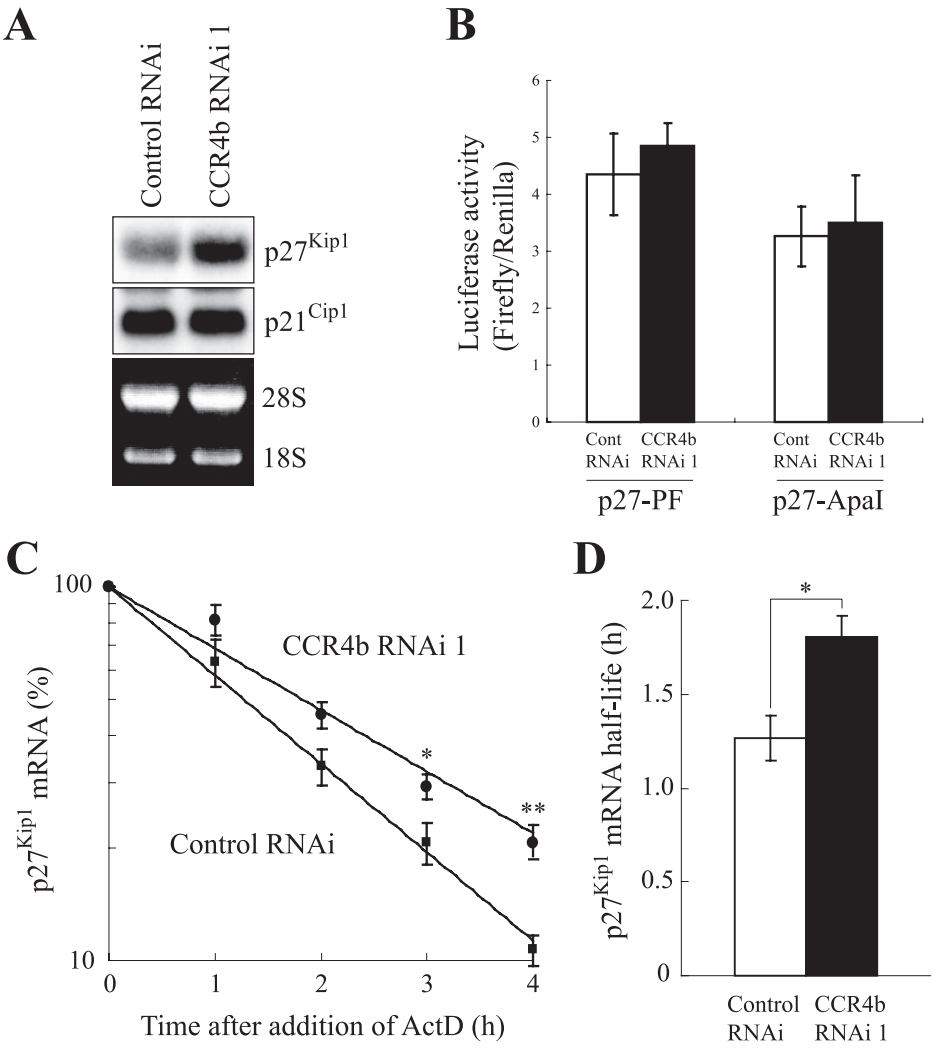

FIG. 8. Elevation of *p27*^{Kip1} mRNA due to its increased stability in CCR4b-depleted cells. (A) Expression of *p27*^{Kip1} and *p21*^{Cip1} mRNAs in NIH 3T3 cells expressing control shRNA and CCR4b shRNA was determined by Northern blot hybridization. Specific cDNAs for *p27*^{Kip1} and *p21*^{Cip1} mRNAs were used as probes. (B) NIH 3T3 cells expressing control shRNA or CCR4b shRNA were transfected with p27-PF and p27-ApaI promoters of the *p27*^{Kip1} gene. Experimental conditions were as described in Materials and Methods. Reporter activities were expressed as ratios of firefly luciferase to *Renilla* luciferase ($n = 3$). The error bars represent standard deviations. $P > 0.5$; Student's *t* test. (C) NIH 3T3 cells (number) infected with CCR4b shRNA virus or control shRNA virus were incubated with actinomycin D (2.5 mg/ml) for the indicated times. The level of *p27*^{Kip1} mRNA was determined by Northern blot hybridization. The amounts of *p27*^{Kip1} mRNA on Northern blots were quantified, normalized to that of *GAPDH* mRNA, and plotted semilogarithmically. Data representative of three experiments are expressed as the percentage relative to the amount of *p27*^{Kip1} mRNA at time zero ($n = 3$). The error bars represent standard deviations. *, $P < 0.01$; **, $P < 0.001$; Student's *t* test. (D) The half-life of *p27*^{Kip1} mRNA was obtained from panel B. The error bars represent standard deviations. *, $P < 0.01$; Student's *t* test.

well known that the 3′ UTR renders *p27*^{Kip1} mRNA unstable (11, 24) and that ARE mediates a deadenylation-dependent decay (5, 15). Therefore, our data strongly suggest that CCR4b is involved in the deadenylation-dependent degradation of *p27*^{Kip1} mRNA in vivo.

The important question as to the mechanism by which CCR4b recognizes target mRNAs remains unanswered. Deadenylation of mRNAs is likely to be regulated by many factors, including deadenylases, poly(A)-binding protein (PABP), translation factors, and RNA-binding proteins (34). CCR4 deadenylase activity is inhibited by PABP (31). In contrast, UNR, an RNA-binding protein, promotes deadenylation of the c-*fos* transcript (4). Although RNA-binding proteins responsible for the rapid degradation of *p27*^{Kip1} mRNA have not been identified, ARE in the 3′ UTR of *p27*^{Kip1} mRNA promotes degradation of *p27*^{Kip1} mRNA (11, 24). Some AREs requires PARN, another deadenylase in mammals (10). Therefore, it is possible that a factor that recognizes the specific sequences in *p27*^{Kip1} mRNA may mediate deadenylation of *p27*^{Kip1} mRNA by interacting with CCR4b. We found by protein purification analysis that mRNA-binding proteins are included in the CCR4-NOT complex (unpublished data). Future studies are needed to identify specific mRNA-binding proteins that influence the deadenylation of CCR4b target mRNAs.

The biological significance of the CCR4-NOT-associated deadenylase activity has been obscure. By examining CCR4b-regulated gene expression profiles comprehensively by DNA microarray analyses (Fig. 7), we have found that, among cell

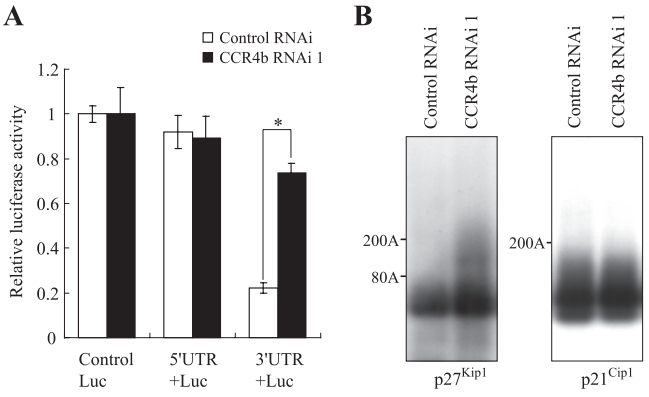

FIG. 9. CCR4b regulates the poly(A) tail of *p27Kip1* mRNA through its 3′ UTR. (A) $p27^{Kip1}$ expression is regulated through its 3′ UTR by CCR4b. NIH 3T3 cells expressing control shRNA or CCR4b shRNA were transfected with Luc, 5′ UTR plus Luc, and Luc plus 3′ UTR. The experimental conditions were as described in Materials and Methods. Reporter activities were expressed as ratios of firefly luciferase to *Renilla* luciferase ($n = 3$). The error bars represent standard deviations. *, $P < 0.001$; Student's t test. (B) PAT assays were performed to measure PATs of *p27Kip1* and *p21Cip1* mRNAs in control and CCR4b-depleted cells. The experimental conditions were as described in Materials and Methods.

cycle-related genes whose expression levels are significantly increased, *p27Kip1* mRNA expression is increased in the CCR4b-depleted cells (Table 1). With this result, we consider that $p27^{Kip1}$ is the most plausible cause of the cell cycle arrest in CCR4b-depleted cells. In other words, $p27^{Kip1}$ is accumulated in the absence of CCR4b, which could result in the inhibition of G_1 cyclin/CDK activity, leading to G_0/G_1 arrest. This would explain the reduction of *cyclin* mRNA expression in CCR4b-depleted cells. Our study provides the first evidence that CCR4b deadenylase regulates the stability of a specific mRNA associated with cell cycle progression and is thereby involved in growth control of mammalian cells.

In conclusion, we showed that in mammals, the CCR4 family protein CCR4b contributes to cell growth through its deadenylase activity. Deadenylases may also play roles in other biological processes, such as embryogenesis, differentiation, and development. In *D. melanogaster*, reduced expression of CCR4 leads to female sterility (17, 29) and embryonic lethality (37), and deletion of CAF1a/CNOT7 leads to male sterility in mice (1, 20). These phenotypes are likely to be caused, at least in part, by changes in gene expression due to altered stability and/or translational efficiency of specific mRNAs, although transcriptional regulation contributes greatly to the latter scenario. Further studies of the CCR4-NOT complex may clarify the contributions of CCR4b deadenylase activity in various physiologic processes.

ACKNOWLEDGMENTS

This work was supported by a grant-in-aid from the Japan Society for the Promotion of Science and from the Ministry of Education, Culture, Sports, Science, and Technology, Japan.

We thank T. Sakai for p27-PF and p27-ApaI plasmids; L. Hengst for 5′ UTR plus Luc and Luc plus 3′ UTR; T. Nagase (Kazusa DNA Research Institute) for the human KIAA1194 cDNA construct; M. Horiuchi for kind advice on the nuclease assay; H. Fukuda for help in mass analysis; and R. F. Whittier, T. Tezuka, and T. Nakazawa for valuable discussions.

REFERENCES

1. **Berthet, C., A. M. Morera, M. J. Asensio, M. A. Chauvin, A. P. Morel, F. Dijoud, J. P. Magaud, P. Durand, and J. P. Rouault.** 2004. CCR4-associated factor CAF1 is an essential factor for spermatogenesis. Mol. Cell. Biol. **24:**5808–5820.
2. **Brown, C. E., and A. B. Sachs.** 1998. Poly(A) tail length control in *Saccharomyces cerevisiae* occurs by message-specific deadenylation. Mol. Cell. Biol. **18:**6548–6559.
3. Reference deleted.
4. **Chang, T. C., A. Yamashita, C. Y. Chen, Y. Yamashita, W. Zhu, S. Durdan, A. Kahvejian, N. Sonenberg, and A. B. Shyu.** 2004. UNR, a new partner of poly(A)-binding protein, plays a key role in translationally coupled mRNA turnover mediated by the c-fos major coding-region determinant. Genes Dev. **18:**2010–2023.
5. **Chen, C. Y., F. Del Gatto-Konczak, Z. Wu, and M. Karin.** 1998. Stabilization of interleukin-2 mRNA by the c-Jun NH2-terminal kinase pathway. Science **280:**1945–1949.
6. **Chen, J., Y. C. Chiang, and C. L. Denis.** 2002. CCR4 3′-5′ poly(A) RNA and ssDNA exonuclease, is the catalytic component of the cytoplasmic deadenylase. EMBO J. **21:**1414–1426.
7. **Chen, J., J. Rappsilber, Y. C. Chiang, P. Russell, M. Mann, and C. L. Denis.** 2001. Purification and characterization of the 1.0 MDa CCR4-NOT complex identifies two novel components of the complex. J. Mol. Biol. **314:**683–694.
8. **Collart, M. A.** 2003. Global control of gene expression in yeast by the Ccr4-Not complex. Gene **313:**1–16.
9. **Denis, C. L., and J. Chen.** 2003. The CCR4-NOT complex plays diverse roles in mRNA metabolism. Prog. Nucleic Acid Res. Mol. Biol. **73:**221–250.
10. **Gao, M., C. J. Wilusz, S. W. Peltz, and J. Wilusz.** 2001. A novel mRNA-decapping activity in HeLa cytoplasmic extracts is regulated by AU-rich elements. EMBO J. **20:**1134–1143.
11. **Gopfert, U., M. Kullmann, and L. Hengst.** 2003. Cell cycle-dependent translation of p27 involves a responsive element in its 5′-UTR that overlaps with a uORF. Hum. Mol. Genet. **12:**1767–1779.
12. **Grosset, C., C. Y. Chen, N. Xu, N. Sonenberg, H. Jacquemin-Sablon, and A. B. Shyu.** 2000. A mechanism for translationally coupled mRNA turnover: interaction between the poly(A) tail and a c-fos RNA coding determinant via a protein complex. Cell **103:**29–40.
13. **Kamiyama, J., T. Inoue, N. Ohtani-Fujita, S. Minami, H. Yamagishi, and T. Sakai.** 1999. The ubiquitous transcription factor NF-Y positively regulates the transcription of human p27Kip1 through a CCAAT box located in the 5-upstream region of the p27Kip1 gene. FEBS Lett. **455:**281–285.
14. **Kawamura-Tsuzuku, J., T. Suzuki, Y. Yoshida, and T. Yamamoto.** 2004. Nuclear localization of Tob is important for regulation of its antiproliferative activity. Oncogene **23:**6630–6638.
15. **Lai, W. S., E. Carballo, J. R. Strum, E. A. Kennington, R. S. Phillips, and P. J. Blackshear.** 1999. Evidence that tristetraprolin binds to AU-rich elements and promotes the deadenylation and destabilization of tumor necrosis factor alpha mRNA. Mol. Cell. Biol. **19:**4311–4323.
16. **Liu, H. Y., V. Badarinarayana, D. C. Audino, J. Rappsilber, M. Mann, and C. L. Denis.** 1998. The NOT proteins are part of the CCR4 transcriptional complex and affect gene expression both positively and negatively. EMBO J. **17:**1096–1106.
17. **Morris, J. Z., A. Hong, M. A. Lilly, and R. Lehmann.** 2005. twin, a CCR4 homolog, regulates cyclin poly(A) tail length to permit *Drosophila* oogenesis. Development **132:**1165–1174.
18. **Muhlrad, D., and R. Parker.** 2005. The yeast EDC1 mRNA undergoes deadenylation-independent decapping stimulated by Not2p, Not4p, and Not5p. EMBO J. **24:**1033–1045.
19. **Mulder, K. W., G. S. Winkler, and H. T. Timmers.** 2005. DNA damage and replication stress induced transcription of RNR genes is dependent on the Ccr4-Not complex. Nucleic Acids Res. **33:**6384–6392.
20. **Nakamura, T., R. Yao, T. Ogawa, T. Suzuki, C. Ito, N. Tsunekawa, K. Inoue, R. Ajima, T. Miyasaka, Y. Yoshida, A. Ogura, K. Toshimori, T. Noce, T. Yamamoto, and T. Noda.** 2004. Oligo-astheno-teratozoospermia in mice lacking Cnot7, a regulator of retinoid X receptor beta. Nat. Genet. **36:**528–533.
21. **Nakazawa, T., A. M. Watabe, T. Tezuka, Y. Yoshida, K. Yokoyama, H. Umemori, A. Inoue, S. Okabe, T. Manabe, and T. Yamamoto.** 2003. p250GAP, a novel brain-enriched GTPase-activating protein for Rho family GTPases, is involved in the *N*-methyl-D-aspartate receptor signaling. Mol. Biol. Cell **14:**2921–2934.
22. **Parker, R., and H. Song.** 2004. The enzymes and control of eukaryotic mRNA turnover. Nat. Struct. Mol. Biol. **11:**121–127.
23. **Sachs, A. B., P. Sarnow, and M. W. Hentze.** 1997. Starting at the beginning, middle, and end: translation initiation in eukaryotes. Cell **89:**831–838.
24. **Sakakibara, K., K. Kubota, B. Worku, E. J. Ryer, J. P. Miller, A. Koff, K. C. Kent, and B. Liu.** 2005. PDGF-BB regulates p27 expression through ERK-dependent RNA turn-over in vascular smooth muscle cells. J. Biol. Chem. **280:**25470–25477.
25. **Salles, F. J., W. G. Richards, and S. Strickland.** 1999. Assaying the polyadenylation state of mRNAs. Methods **17:**38–45.

26. **Seimiya, H., and S. Smith.** 2002. The telomeric poly(ADP-ribose) polymerase, tankyrase 1, contains multiple binding sites for telomeric repeat binding factor 1 (TRF1) and a novel acceptor, 182-kDa tankyrase-binding protein (TAB182). J. Biol. Chem. **277:**14116–14126.
27. **Sherr, C. J., and J. M. Roberts.** 1999. CDK inhibitors: positive and negative regulators of G_1-phase progression. Genes Dev. **13:**1501–1512.
28. **Suzuki, T., K.-J. Tsuzuku, R. Ajima, T. Nakamura, Y. Yoshida, and T. Yamamoto.** 2002. Phosphorylation of three regulatory serines of Tob by Erk1 and Erk2 is required for Ras-mediated cell proliferation and transformation. Genes Dev. **16:**1356–1370.
29. **Temme, C., S. Zaessinger, S. Meyer, M. Simonelig, and E. Wahle.** 2004. A complex containing the CCR4 and CAF1 proteins is involved in mRNA deadenylation in *Drosophila*. EMBO J. **23:**2862–2871.
30. **Traven, A., A. Hammet, N. Tenis, C. L. Denis, and J. Heierhorst.** 2005. Ccr4-Not complex mRNA deadenylase activity contributes to DNA damage responses in *Saccharomyces cerevisiae*. Genetics **169:**65–75.
31. **Tucker, M., M. A. Valencia-Sanchez, R. R. Staples, J. Chen, C. L. Denis, and R. Parker.** 2001. The transcription factor associated CCR4 and Caf1 proteins are components of the major cytoplasmic mRNA deadenylase in *Saccharomyces cerevisiae*. Cell **104:**377–386.
32. **Viswanathan, P., T. Ohn, Y. C. Chiang, J. Chen, and C. L. Denis.** 2004. Mouse CAF1 can function as a processive deadenylase/3′-5′-exonuclease in vitro but in yeast the deadenylase function of CAF1 is not required for mRNA poly(A) removal. J. Biol. Chem. **279:**23988–23995.
33. **Westmoreland, T. J., J. R. Marks, J. A. Olson, Jr., E. M. Thompson, M. A. Resnick, and C. B. Bennett.** 2004. Cell cycle progression in G_1 and S phases is CCR4 dependent following ionizing radiation or replication stress in *Saccharomyces cerevisiae*. Eukaryot. Cell **3:**430–446.
34. **Wilusz, C. J., M. Wormington, and S. W. Peltz.** 2001. The cap-to-tail guide to mRNA turnover. Nat. Rev. Mol. Cell Biol. **2:**237–246.
35. **Yamashita, A., T. C. Chang, Y. Yamashita, W. Zhu, Z. Zhong, C. Y. Chen, and A. B. Shyu.** 2005. Concerted action of poly(A) nucleases and decapping enzyme in mammalian mRNA turnover. Nat. Struct. Mol. Biol. **12:**1054–1063.
36. **Yoshida, Y., S. Tanaka, H. Umemori, O. Minowa, M. Usui, N. Ikematu, E. Hosoda, T. Imamura, J. Kuno, T. Yamashita, K. Miyazono, M. Noda, T. Noda, and T. Yamamoto.** 2000. Negative regulation of BMP/Smad signaling by Tob in osteoblasts. Cell **103:**1085–1097.
37. **Zaessinger, S., I. Busseau, and M. Simonelig.** 2006. Oskar allows nanos mRNA translation in *Drosophila* embryos by preventing its deadenylation by Smaug/CCR4. Development **133:**4573–4583.